ELSEVIER

Coordination Chemistry Reviews 226 (2002) 251–259

COORDINATION CHEMISTRY REVIEWS

www.elsevier.com/locate/ccr

Theoretical study on kinetic isotope effects in the C–H bond activation of alkanes by iron-oxo complexes

Kazunari Yoshizawa *

Institute for Fundamental Research of Organic Chemistry, Kyushu University, Fukuoka 812-8581, Japan

Received 16 April 2001; received in revised form 11 October 2001; accepted 22 November 2001

Contents

Abstract

The C–H bond dissociation reactions of methane and ethane by the bare FeO^+ complex, diiron and dicopper models of methane monooxygenase, and a compound I model of cytochrome P450 are discussed using density functional theory (DFT) calculations, with an emphasis on their kinetic isotope effects (KIEs). There are possible three types of transition states for the C–H bond dissociation. The first is an oxene insertion mechanism, in which a C–H bond is dissociated and C–O and O–H bonds are formed in a concerted manner via a three-centered transition state C···H···O–Fe which directly leads to a product alcohol. The second is a direct abstraction mechanism in which a linear transition state C···H···O–Fe leads to the dissociation into an Fe–OH intermediate and an alkyl radical species. The third mechanism involves a four-centered transition state C···H···O–Fe in its initial stages, which leads to a reaction intermediate involving OH and CH_3 ligands. DFT computations demonstrate that the second and third types of transition states are likely to occur in the activation of a C–H bond. The four-centered H atom abstraction can preferentially occur when the metal active center of catalysts and enzymes is coordinatively unsaturated (five-coordinate), whereas the direct abstraction should occur when the metal active center is six-coordinate. KIE values calculated with transition state theory are significantly dependent on temperature, substituents, and ways of abstraction.

Keywords: Kinetic isotope effect; C–H bond activation; Cytochrome P450; Methane monooxygenase; Transition state theory; Density functional theory

1. Introduction

The mechanism of selective alkane oxidation by various iron-oxo species has been extensively investigated, mainly with the development of a high-performance catalytic system in mind. Cytochrome P450 [1,2] and methane monooxygenase [3,4] are well-known enzymes that are able to catalyze the addition of molecular oxygen to nonactivated hydrocarbons under physiological conditions. The active electrophilic oxidant in P450 has been assumed to be an oxo-ferryl ($O = Fe^{IV}$) porphyrin π-cation radical which is called compound I.

* Tel.: +81-92-642-2720; fax: +81-92-642-2735.
E-mail address: kazunari@ms.ifoc.kyushu-u.ac.jp (K. Yoshizawa).

0010-8545/02/$ - see front matter
PII: S0010-8545(01)00464-7

The essential reaction involves a C–H bond dissociation and an oxygen insertion into the C–H bond to produce an alcohol C–O–H. Replacement of the hydrogen atom with deuterium can lead to a significant isotope effect in the reaction rate, which is referred to as a kinetic isotope effect (KIE)k_H/k_D. The magnitude of the isotope effect provides important information with respect to the mechanism of hydroxylation reactions in which the C–H bond cleavage is believed to be the rate-determining step. According to the pioneering work of Hjelmeland et al. [5] and Groves et al. [6], observed KIEs are large; $k_H/k_D > 11$ for benzylic hydroxylation and aliphatic hydroxylation. KIE experiments have been extensively carried out for the past two decades [7]. Observed large isotope effects strongly support the 'oxygen rebound' mechanism [8], in which the iron-oxo species directly abstracts an H atom from substrate to give an iron-hydroxo intermediate and an alkyl radical species, followed by recombination of these species and release of a product alcohol.

Methane monooxygenase (MMO) [3,4], which exists in some methanotrophs as an iron-containing soluble form (sMMO) and a copper-containing membrane form (pMMO), catalyzes methane hydroxylation using molecular oxygen under physiological conditions. A key intermediate **Q** of sMMO, the species responsible for the direct reactivity toward methane, has been proposed to involve a high-valent dinuclear Fe(IV) complex [9,10]. It was suggested from Mössbauer and EXAFS analyses that the active site of intermediate **Q** should involve an $Fe_2(\mu\text{-}O)_2$ diamond core [11]. Particulate MMO (pMMO) is a copper-containing membrane protein [12], but in contrast to sMMO, the structure of the pMMO active site is unknown at present because of difficulty in handling purified pMMO. In both *Metylococcus capsulatus* (Bath) and *Metylosinus trichosporium* OB3b, methane oxidation is carried out mostly by sMMO under conditions of copper limitation; however, addition of copper to the growth medium significantly increases the activity of pMMO. Although the role of copper in the pMMO activity is still not fully understood, copper should play a role in methane oxidation by pMMO.

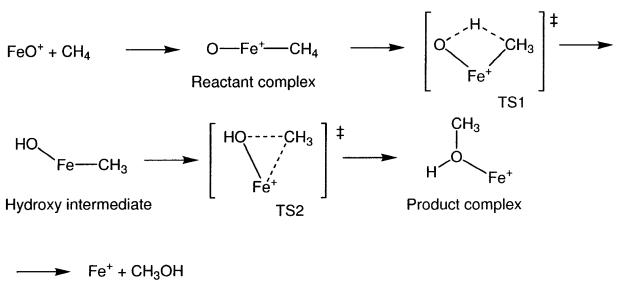

Fig. 1. Mechanism for the methane–methanol conversion by the bare FeO^+ complex.

Schröder, Schwarz and coworkers [13–15] discovered the gas-phase reaction, $FeO^+ + CH_4 \rightarrow Fe^+ + CH_3OH$, which occurs under ion-cyclotron-resonance conditions. One of the most important aspects of the FeO^+-mediated hydroxylation reaction is the 'two-state reactivity' in which closely lying high- and low-spin potential energy surfaces result in the occurrence of spin inversion [16]. Although the oxidation state of the iron atom in FeO^+ is different from that of the enzymatic systems, this simple methane hydroxylation is probably a key to a better understanding of the role of iron-oxo species in the active intermediates of P450 and sMMO. In fact, the mechanism and energetics of this reaction has been well investigated in terms of mass spectrometric analyses and density functional theory (DFT) calcuations. We have proposed an addition–elimination reaction pathway [17,18] for the methane to methanol conversion by the bare FeO^+ complex. Our proposal for the reaction is indicated in Fig. 1: (1) in the initial stages of the reaction, C_{3v}- or D_{2d}-distorted methane is activated on the coordinatively unsaturated iron-oxo complex to form a methane complex; (2) abstraction of an H atom of methane occurs via the four-centered transition state (TS1) leading to a reaction intermediate that involves resultant OH and CH_3 ligands; (3) concerted methyl migration via the three-centered transition state (TS2) finally leads to a methanol complex. An essential feature of this mechanism is that no alkyl radical is formed in the course of the reaction pathway. Detailed energetics for methane hydroxylation by $ScO^+ \sim CuO^+$ is given in a previous paper [18]. For example, the ground sextet state of FeO^+ lies 5.8 kcal mol^{-1} below the lowest quartet state whereas TS1 of the sextet state lies 9.0 kcal mol^{-1} above TS1 of the quartet state. As a result, spin inversion should occur during the C–H bond dissociation. We have proposed that this mechanism is applicable to methane hydroxylation by sMMO [19–21] and the direct conversion of benzene to phenol by FeO^+ [22] and Fe-ZSM-5 zeolite [23].

Quantum chemical calculations have recently provided useful information with respect to the mechanistic aspects of P450 [24,25] and MMO [26–28]. Various mechanisms of these enzymes are discussed from different viewpoints in these papers. One of the most important data obtained from theoretical calculations is KIEs for C–H bond activation, by which we can deepen our understanding of the mechanism of hydroxylation. In previous studies [20,29,30], we have calculated and analyzed KIEs in the processes of H atom abstraction by various iron-oxo species. In this review, we turn our attention to the C–H bond activation of methane and ethane by the bare FeO^+ complex, sMMO, pMMO, and P450.

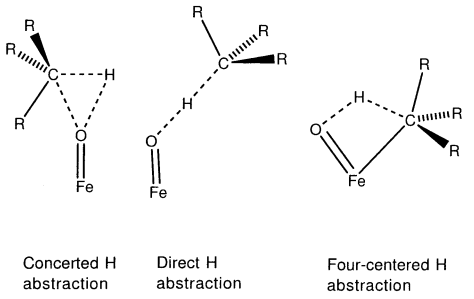

Fig. 2. Possible mechanisms for C–H bond cleavage of alkane.

2. Method of calculation

KIE values were calculated from transition state theory [31] with Eq. (1),

$$\frac{k_{\mathrm{H}}}{k_{\mathrm{D}}} = \left(\frac{m^{\mathrm{R}}_{\mathrm{D\text{-}form}} m^{\#}_{\mathrm{H\text{-}form}}}{m^{\mathrm{R}}_{\mathrm{H\text{-}form}} m^{\#}_{\mathrm{D\text{-}form}}}\right)^{3/2} \left(\frac{I^{\mathrm{R}}_{x\mathrm{D\text{-}form}} I^{\mathrm{R}}_{y\mathrm{D\text{-}form}} I^{\mathrm{R}}_{z\mathrm{D\text{-}form}}}{I^{\mathrm{R}}_{x\mathrm{H\text{-}form}} I^{\mathrm{R}}_{y\mathrm{H\text{-}form}} I^{\mathrm{R}}_{z\mathrm{H\text{-}form}}}\right)^{1/2} \times \left(\frac{I^{\#}_{x\mathrm{H\text{-}form}} I^{\#}_{y\mathrm{H\text{-}form}} I^{\#}_{z\mathrm{H\text{-}form}}}{I^{\#}_{x\mathrm{D\text{-}form}} I^{\#}_{y\mathrm{D\text{-}form}} I^{\#}_{z\mathrm{D\text{-}form}}}\right)^{1/2} \frac{q^{\mathrm{R}}_{\mathrm{vD\text{-}form}} q^{\#}_{\mathrm{vH\text{-}form}}}{q^{\mathrm{R}}_{\mathrm{vH\text{-}form}} q^{\#}_{\mathrm{vD\text{-}form}}} \exp\left(-\frac{E^{\#}_{\mathrm{H\text{-}form}} - E^{\#}_{\mathrm{D\text{-}form}}}{RT}\right) \quad (1)$$

where superscripts R and # specify the reactant and the transition state, respectively, for the molecular mass m, the moment of inertia I, the vibrational partition function q_{v}, and the activation energy E. Transition states were optimized and characterized from vibrational analyses; they were confirmed to have only one imaginary mode of vibration. The last exponential term in this equation tells us that KIEs are temperature dependent. The numerator in the last exponential term comes from the fact that the C–H bond dissociation has a lower activation energy than the C–D dissociation on account of the former's greater zero-point vibrational energy. Wigner's tunneling corrections [32] were added to KIE values obtained from transition state theory; the correction coefficient κ is written in the form of $1\text{-}1/24(hv^{\ddagger}/kT)^2$, where $v^{\ddagger}$ is the imaginary frequency relevant to a transition state. These quantities are correctly obtained from DFT calculations. We used the B3LYP method [33,34], a hybrid Hartree–Fock/DFT method in obtaining the geometries, energies, and vibrational frequencies of reaction species.

3. Results and discussion

3.1. Possible mechanisms for C–H bond dissociation

Let us first look at how an H atom of substrate is abstracted by an iron-oxo species. Fig. 2 shows that there are three possible transition states for the cleavage of a C–H bond. In the first mechanism indicated at the left, one C–H bond is dissociated and C–O and O–H bonds are formed at the same time, leading to a product alcohol. This concerted 'oxene insertion' mechanism was proposed in an earlier study of the mechanism of P450-catalyzed hydroxylation [35]. Newcomb and collaborators proposed from their radical clock studies a side-on direct insertion of oxygen to a C–H bond which is similar to the oxene insertion mechanism [36]. In the second mechanism indicated at the center, the iron-oxo species abstracts an H atom from substrate to give an iron-hydroxo intermediate and an alkyl radical species, followed by rapid transfer of the iron-bound hydroxyl radical to the alkyl radical. This type of H atom abstraction is widely believed to take place in the initial stages of the so-called oxygen rebound mechanism [1,2]. Observed large KIEs and loss of stereochemistry in P450-catalyzed hydroxylation reactions prefer a nonconcerted mechanism to the concerted oxene insertion mechanism mentioned above. The four-centered H atom abstraction indicated at the right was proposed to occur in methane hydroxylation by the bare FeO^+ complex [17,18]. This is clearly different from the direct abstraction mechanism in that there is a significant interaction between the iron active center and a carbon atom of substrate in the four-centered abstraction. No alkyl radical species is formed in this mechanism because the carbon atom is bound to the coordinatively unsaturated iron after the H atom abstraction is completed; see Fig. 1.

We obtained both second and third types of transition states from DFT calculations for the CH_4/FeO^+ system [37]; the direct abstraction, which occurs only in the high-spin sextet state, is energetically less favorable than the four-centered abstraction, due to the lack of the Fe···C interaction. Therefore the four-centered abstraction can preferentially take place when the metal active center of catalysts and enzymes is coordinatively unsaturated. On the other hand, we failed to optimize the transition state for the concerted oxene insertion despite our best efforts. This result is reasonable because a carbon atom of alkanes is four-coordinate and therefore the oxo group cannot attack a specific C–H bond from a geometrical point of view. In this paper we discuss KIE calculational results on the direct abstraction and the four-centered abstraction. We consider the C–H bond dissociation of methane by the bare FeO^+ complex and diiron and dicopper models of methane monooxygenase and that of ethane by a compound I model of cytochrome P450.

3.2. C–H bond activation by the bare FeO^+ complex

Fig. 3 shows optimized transition-state structures for the four-centered abstraction and the direct abstraction [37], which we call TS1 and TSd, respectively. The four-centered abstraction via TS1 leads to the hydroxo

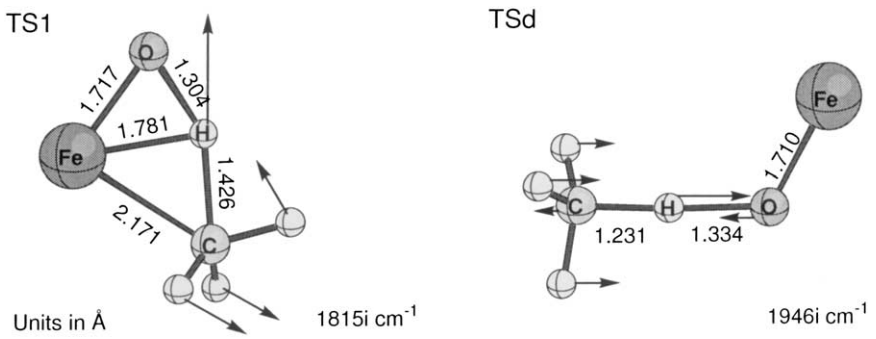

Fig. 3. Optimized transition states for the four-centered abstraction (TS1) and the direct abstraction (TSd) in the FeO^+/CH_4 system. An imaginary frequency mode is related with each transition state.

intermediate HO–Fe^+–CH_3, which is converted to complex $Fe^+(CH_3OH)$ through the recombination of the OH and the CH_3 ligands on the iron active site. In contrast, the direct abstraction via TSd exhibits a nearly linear C–H–O array, as expected from a conventional radical mechanism. The direct abstraction occurs only in the high-spin sextet state whereas the four-centered abstraction occurs in both low-spin quartet and high-spin sextet states. The imaginary mode indicated in TSd clearly tells us that this transition state is responsible for the dissociation into the Fe^+OH and $^{\bullet}CH_3$ fragments. TSd of the sextet state lies 4.5 kcal mol^{-1} above TS1 of the quartet state. We therefore concluded that such a direct H atom abstraction is unlikely to occur at least in the gas-phase methane activation by the bare FeO^+ complex.

To aid our understanding of the two kinds of H atom abstractions, it is useful to look at fragment molecular orbital (FMO) analyses. In the FMO method we do not need to know the details of the electronic structures of the fragments; it is sufficient that we look at the frontier orbitals of the fragments and their reconstruction. The molecular orbitals of the FeO^+ fragment are indicated at the center in Fig. 4. The 2σ and 1π orbitals are localized mainly on the oxygen atom, but the 1δ, 2π, and 3σ are localized more on the iron atom; thus, the 1δ, 2π, and 3σ can be viewed as d-block orbitals. The orbital interactions for TS1 and TSd are indicated to the left and right, respectively. In TS1 the 3σ orbital of the FeO^+ fragment is significantly pushed up to -10.5 eV due to an interaction with the '$t_2(1)$' HOMO of the CH_4 fragment, and therefore the sextet state of TS1 is energetically unstable within the framework of one-electron theory. In contrast to the sextet state, TS1 in the low-spin quartet state can be stabilized because the destabilized orbital at -10.5 eV is not filled in the quartet state. On the other hand, TS1 should be greatly stabilized in the quintet state of FeO^{2+}, a d^4 complex, because the destabilized 3σ is unfilled in this state and exchange interactions among the four electrons housed in the four low-lying d-block orbitals can work reasonably well to stabilize the quintet state of FeO^{2+}. This prediction is correct from DFT computations [37].

Let us next find a good reason why the direct H atom abstraction occurs only in the sextet state of FeO^+. As shown in the FMO analysis for TSd at the right in Fig. 4, the a_1 HOMO of the CH_4 fragment interacts with the 2σ and 1π of the FeO^+ fragment that are localized mainly on the oxygen atom. The electronic structure of TSd is expected to be greatly stabilized in the sextet state because all the d-block orbitals lying within a range of -12.6 to -11.8 eV are singly occupied and consequently exchange interactions can work well among the five electrons with the same spin housed in the close-lying five d-block orbitals.

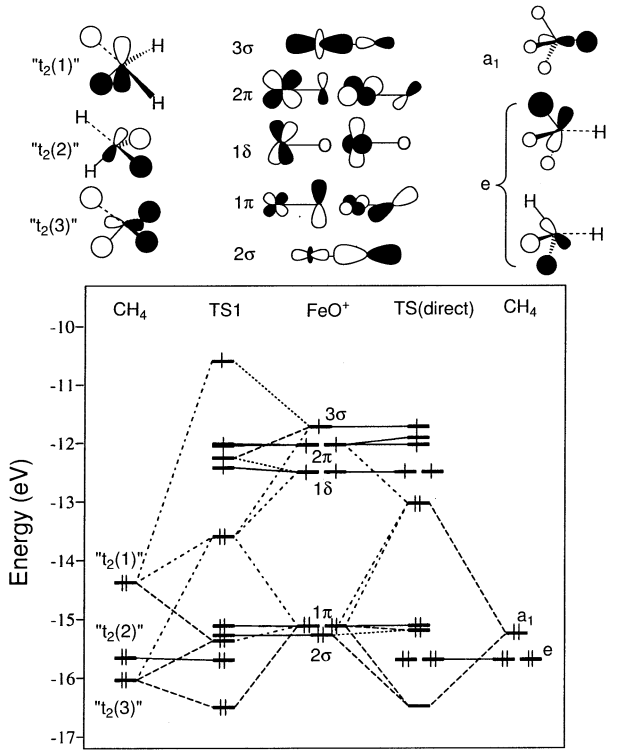

Fig. 4. FMO analyses for TS1 and TSd in the sextet state of FeO^+.

Table 1
KIE values in the C–H bond dissociation of methane by the bare FeO^+ complex

T (K)	TS1(^{6}A)	TS1(^{4}A)	TSd(^{6}A)
200	19.70 (33.95)	19.11 (29.78)	40.52 (67.02)
250	13.08 (21.53)	12.61 (18.54)	23.57 (37.55)
300	9.72 (15.29)	9.37 (13.06)	16.05 (24.62)
350	7.70 (11.57)	7.44 (9.90)	11.94 (17.63)
400	6.36 (9.17)	6.16 (7.88)	9.40 (13.39)

The values in parentheses include Wigner's tunneling correction.

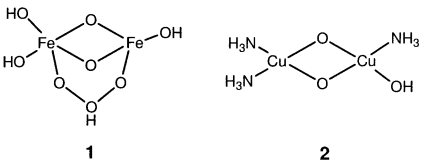

1 2

Fig. 5. Diiron and dicopper active site models of MMO.

Table 1 summarizes calculated values of k_H/k_D for the four-centered abstraction via TS1 of both sextet and quartet states and for the direct abstraction via TSd of the sextet state in the $FeO^+/CH_4(CD_4)$ system as a function of temperature [27]. At 300 K, the value for TS1 is 9.72 and 9.37 in the sextet and the quartet states, respectively, and that for TSd is 16.05 in the sextet state. As expected and calculated, Wigner's tunneling corrections significantly enhance the isotope effects. The predicted isotope effect is more significant in the direct abstraction than in the four-centered abstraction.

3.3. C–H bond activation by diiron and dicopper models of MMO

Some mechanistic proposals for methane hydroxylation by intermediate **Q** of sMMO were reported a few years ago [38–44]. More recent experimental and theoretical studies with respect to the mechanistic aspects of sMMO were summarized [45]. According to this review, the following issues remain unsolved: (1) the structure of the true active intermediate that has the direct reactivity to methane, (2) relevance between a bis(μ-oxo)diiron(IV) structure and intermediate **Q**, (3) whether the iron atoms are coordinatively saturated, or coordinatively unsaturated to allow the formation of an Fe–C bond, (4) involvement of substrate radicals in a mechanism similar to the oxygen rebound mechanism for cytochrome P450, and (5) whether hydroxylation is better described by a concerted mechanism in which an activated oxygen atom inserts directly into a C–H bond. These situations cannot allow us to set up a reasonable model for the active species of sMMO.

Lipscomb, Que, and collaborators suggested from Mössbauer and EXAFS analyses that the active site of intermediate **Q** of sMMO should involve an $Fe_2(\mu\text{-}O)_2$ diamond core [11]. Although X-ray structural analysis has not yet been successful for the key intermediate, the first coordination sphere around each iron atom has been proposed from EXAFS analyses to consist of 4.5 O/N on the average. We set up a diiron model according to these proposals. Relatively little is known about the pMMO active site because of the difficulty of studying membrane-bound proteins and the fact that pMMO is highly unstable, but proposals for the structure of the pMMO active site include trinuclear copper(II) [12], mononuclear copper(II) [46,47], and dinuclear mixed-valent Cu(II)Cu(III) clusters [48]. We adopted a Cu(II)Cu(III) cluster. Our diiron (**1**) and dicopper (**2**) models shown in Fig. 5 are small, but they enable us to carry out systematic vibrational analyses, which will increase the quality of discussions on computed structures and energetics for the reaction pathways [20]. Moreover, these models enable us to calculate KIEs for the C–H cleavage process from vibrational analyses.

Fig. 6 shows optimized structures for the transition states for the four-centered abstraction and the direct abstraction by the diiron complex **1**. The essential features of these are identical to those in the FeO^+/CH_4 system. We found that TSd occurs in the spin undecet ($S = 5$) state while TS1 occurs in broken-symmetry

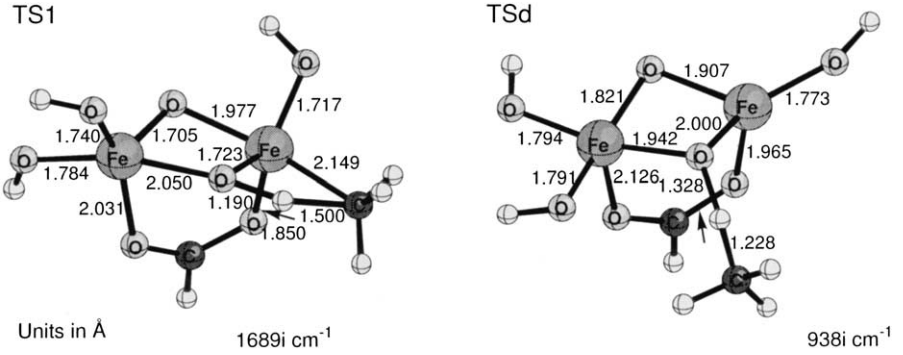

Fig. 6. Optimized transition states for the four-centered H abstraction (TS1) and the direct H abstraction (TSd) from methane by a diiron model of sMMO. An imaginary frequency mode is related with each transition state.

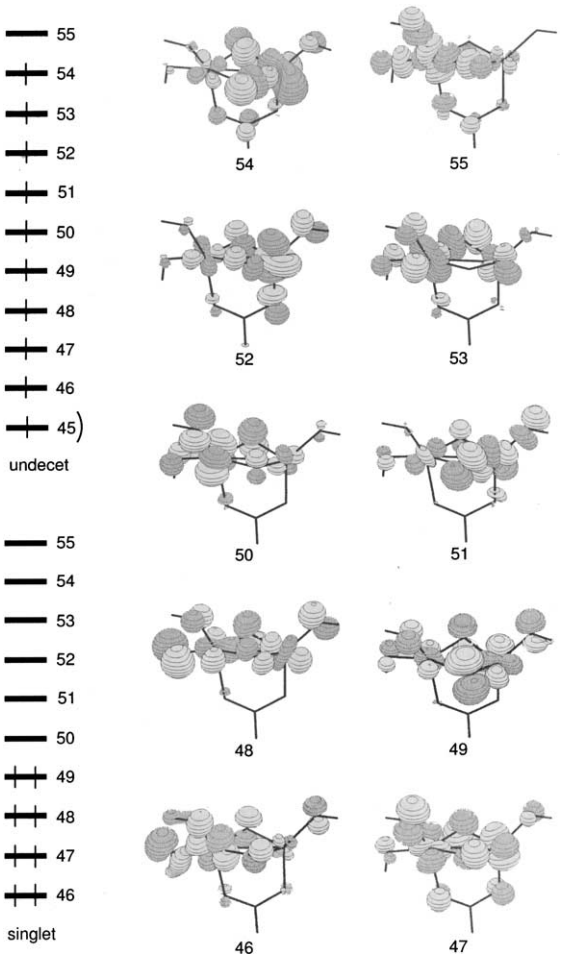

Fig. 7. The d-block orbitals of a diiron model complex.

singlet state calculations. TSd also occurs in the doublet state of **2**. This result arises from the difference in the number of d electrons in the Fe(IV), Cu(II), and Cu(III) ions. If the Fe–O σ* orbitals, the amplitude of which exists on the oxygen atoms in some degree, are singly occupied in the spin undecet state, the radical character of the oxo atoms in **1** increases and plays a major role in the direct H atom abstraction [20]. Fig. 7 shows the d-block orbitals of **1**. Let us consider from these orbitals why the direct H atom abstraction occurs in the undecet state of the diiron complex. In the singlet state the 49th orbital is the HOMO while in the undecet state the 54th orbital is the highest SOMO (singly occupied molecular orbital). Note that the 54th and 55th orbitals are of σ type with respect to an Fe–O bond, and they are similar to the 3σ orbital of the bare FeO^+ complex in Fig. 4. If these σ-type orbitals are singly occupied, the radical character of the oxo species increases; we can expect that the direct H atom abstraction should occur in the undecet state on the analogy of the FeO^+/CH_4 case. Thus, our computational result that the direct H atom abstraction occurs in the undecet state is reasonable in view of the frontier orbitals of the diiron model. The d-block orbitals of **2** are indicated in Fig. 8. The orbitals are simple compared to those of **1**, due to the pseudo-D_{2h} geometry of the diamond core of **2**. Since the number of d electrons is larger in copper, the d-block orbitals of the dicopper model are doubly occupied, except for the highest two orbitals. The 47th and 48th orbitals of **2** are similar to the 54th and 55th orbitals of **1** in that these d-block orbitals are of σ type with respect to the metal–oxygen bonds in the diamond cores. Since in the doublet state of **2** the 47th orbital is the highest SOMO, we expect the direct H atom abstraction to occur in the doublet state of **2**. We therefore think that the direct H atom abstraction should be preferred in the dicopper complex rather than in the diiron complex. In any case, the σ-type orbitals of the dinuclear complexes play an essential role in the direct H atom abstraction of hydrocarbon substrates.

Table 2 summarizes calculated values of k_H/k_D for the four-centered abstraction via TS1 of **1** and **2** and for the direct abstraction via TSd as a function of temperature. At 300 K, TS1 gives k_H/k_D values of 8.62–9.72 while TSd gives k_H/k_D values of 10.59–16.36. In line with the results in the FeO^+/CH_4 system, the

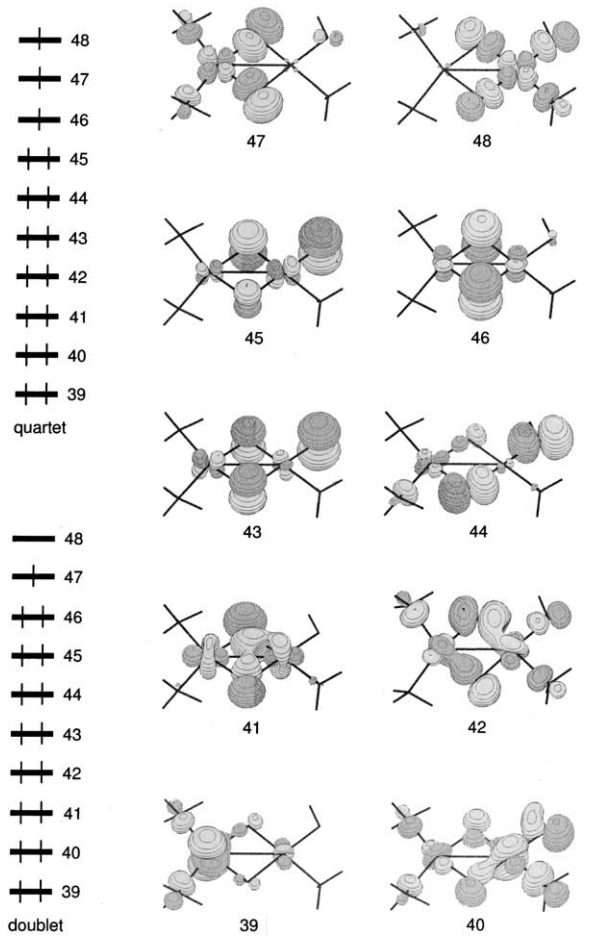

Fig. 8. The d-block orbitals of a dicopper model complex.

Table 2
KIE values in the C–H bond dissociation of methane by sMMO (**1**) and pMMO (**2**) models

T (K)	**1** TS1(^{1}A)	**1** TS1(^{3}A)	**1** TSd(^{11}A)	**2** TS1(^{2}A)	**2** TSd(^{2}A)
200	15.85 (26.52)	17.47 (29.66)	24.33 (33.15)	18.81 (30.68)	45.18 (62.77)
250	11.15 (17.79)	12.08 (19.61)	14.95 (19.24)	12.85 (19.85)	25.00 (32.91)
300	8.62 (13.11)	9.22 (14.30)	10.59 (13.01)	9.72 (14.26)	16.36 (20.57)
350	6.99 (10.17)	7.42 (11.00)	8.11 (9.60)	7.76 (10.86)	11.75 (14.22)
400	5.87 (8.20)	6.19 (8.82)	6.54 (7.52)	6.46 (8.66)	8.96 (10.53)

The values in parentheses include Wigner's tunneling correction.

direct abstraction transition states afford larger values of k_H/k_D than the four-centered transition states. Floss, Lipscomb, and coworkers [49] reported a k_H/k_D value of 4.2 for the hydrogen abstraction in ethane hydroxylation by sMMO isolated from *Methylosinus trichosporium* OB3b. More recently, Neshaim and Lipscomb reported a KIE value of $\sim$50–100 at 4°C for the hydroxylation of CH_4 vs. CD_4 by sMMO [50], while Lippard and coworkers found a similarly large KIE of $\sim$28 at 4°C for the same reaction in sMMO from *Methylococcus capsulatus* (Bath) [51]. Such large KIE values can be explained by a hydrogen tunneling effect. Although the reason for the difference in these experiments is unclear to us, the more recent results suggest that the quantum tunneling effect plays a crucial role in the H atom abstraction.

3.4. C–H bond activation by a compound I model of P450

Shaik and coworkers have suggested from DFT computations that interactions of the substrate with the oxo ligand play a crucial process in alkane hydroxylation by cytochrome P450 [24,25]. They derived some important mechanistic aspects of P450-catalyzed hydroxylation reactions and indicated the participation of two-state reactivity in the C–H bond dissociation process and in the resultant iron-hydroxo intermediate using a compound I model with SH^- as the proximal ligand. One of the most important findings in their studies is that the transition state for the rebound step lies 5 kcal mol^{-1} above the iron-hydroxo species on the high-spin quartet potential energy surface whereas there is no such transition state on the low-spin doublet one. Here we turn our attention to the C–H bond activation by compound I of P450, an iron-oxo porphyrin complex. Only the direct abstraction can occur in our compound I model ($Fe^{+4}O^{-2}(C_{20}N_4H_{12})^{-1}(SCH_3)^{-1}$) since it has a six-coordinate iron active center [29]. An optimized geometry of the transition state for the H-atom abstraction from ethane and the imaginary frequency mode of 1540i cm^{-1} in the quartet state are shown in Fig. 9. The imaginary mode and its high frequency number suggest that this transition state is responsible for the electronic process of the H atom abstraction from ethane. It involves a nearly linear arrangement with respect to the (Fe)O···H···C moiety. The energy difference between the doublet and quartet states of the compound I model is very small, the doublet lying only 0.1 kcal mol^{-1} below the quartet, but the transition state of the doublet state lies 6.4 kcal mol^{-1} above that of the quartet state [29]. So the reaction essentially occurs on the quartet potential energy surface. The activation energy required for the C–H bond cleavage is 21.2 kcal mol^{-1} relative to the dissociation limit on the quartet potential energy surface. We attempted to optimize the transition state for the oxene insertion into a C–H bond of ethane, but we could not obtain such a triangle arrangement indicated at the left of Fig. 2. This is reasonable considering the tetrahedral structure of the carbon atoms of ethane, and we think from this result that the oxene insertion may be an unrealistic mechanism in P450-catalyzed hydroxylation reactions.

Table 3 lists calculated KIE values of k_a/k_b, k_a/k_c, and k_a/k_d, in which k_a is the rate constant for the H atom abstraction from CH_3CH_3, and k_b, k_c, and k_d are those for the D atom abstraction from CDH_2CH_3, CD_3CH_3, and CD_3CD_3, respectively. These values strongly depend on temperature, and it is therefore

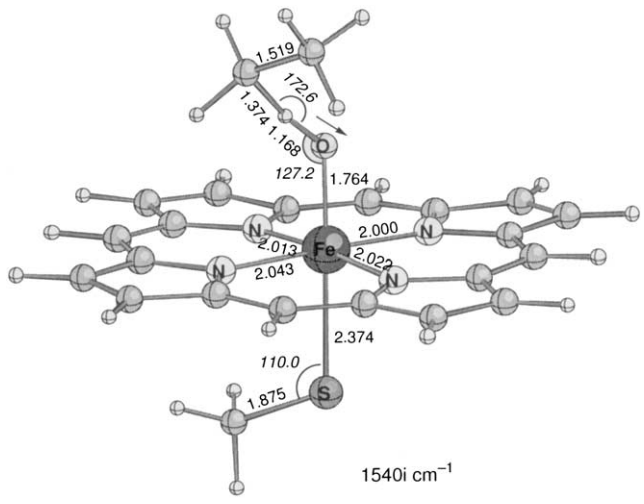

Fig. 9. An optimized transition state for the direct H abstraction (TSd) from ethane by a compound I model of P450. An imaginary frequency mode is related with this transition state.

Table 3
KIE values in the C–H bond dissociation of ethane by a CH_3S^--ligated compound I model

T (K)	k_a/k_b	k_a/k_c	k_a/k_d
^4A			
200	17.15 (27.00)	29.28 (46.87)	39.94 (63.93)
250	10.20 (15.32)	16.42 (25.01)	21.58 (32.51)
300	7.23 (10.37)	11.07 (16.08)	14.16 (20.37)
350	5.64 (7.75)	8.23 (11.44)	10.37 (14.26)
400	4.65 (6.16)	6.51 (8.70)	8.06 (10.07)
^2A			
200	15.45 (21.21)	28.68 (39.88)	36.04 (50.18)
250	9.38 (12.24)	16.11 (21.25)	19.39 (25.61)
300	6.72 (8.40)	10.82 (13.64)	12.68 (16.00)
350	5.29 (6.38)	8.04 (9.76)	9.23 (11.22)
400	4.39 (5.14)	6.33 (7.46)	7.17 (8.46)

k_a is the rate constant for the H-atom abstraction of CH_3CH_3, and k_b, k_c, and k_d are those for the D-atom abstraction of CDH_2CH_3, CD_3CH_3, and CD_3CD_3, respectively. The values in parentheses include Wigner's tunneling correction.

essential to specify temperature conditions in discussing possible reaction mechanisms from measured kinetic isotope data. The variation in the k_a/k_b, k_a/k_c, and k_a/k_d values suggests that KIEs are significantly affected by molecular parts that have no direct relevance to the abstraction reaction. This is simply because the values are significantly dependent on the vibrational structure of a whole molecule. The values calculated from transition state theory fall in a range of 7–14 at 300 K. These quantities are significantly increased with Wigner's tunneling corrections. However, Jones et al. found that the k_H/k_D values of P450 hydroxylation from a few substrates are nearly equal to those of corresponding hydrogen abstraction by *tert*-butoxyl radical and that the k_H/k_D values fall in a range of 2–6 [52]. This may suggest that the rate-determining step in the P450-catalyzed hydroxylation reactions is not the H atom abstraction. In fact, according to the DFT calculations of Shaik and coworkers, the transition state for the rebound step in the quartet state is higher in energy than that for the H atom abstraction [25]. We also obtained a similar result that the transition state for the rebound step lies a few kcal mol^{-1} above the transition state for the H atom abstraction [53].

4. Conclusions

We considered the mechanisms of the C–H bond dissociation reactions of methane by the bare FeO^+ complex, diiron and dicopper models of MMO, and that of ethane by a compound I model of cytochrome P450. DFT calculations demonstrated that there are two types of transition states for the C–H bond dissociation of alkanes. One is a linear transition state which leads to the formation of an Fe–OH intermediate and an alkyl radical species, and the other is a four-centered transition state which leads to a reaction intermediate involving OH and CH_3 ligands. The coordination number of the metal active center can determine which mechanism actually takes place. The four-centered process is preferred at a coordinatively unsaturated metal active center whereas the direct abstraction process is preferred at a six-coordinate metal active center. We think whether the iron atoms coordinatively saturated, or unsaturated to allow the formation of an Fe–C bond is a key issue in discussing the mechanism of hydroxylation reactions. Our calculations demonstrated that the four-centered H atom abstraction can occur in MMO-catalyzed hydroxylation reactions if the diiron active centers of intermediate **Q** are coordinatively unsaturated (five-coordinate). However, the oxygen rebound mechanism is a reasonable hypothesis for P450-catalyzed hydroxylation reactions in the H atom abstraction step because the active species of P450 (compound I) is a six-coordinate iron-oxo species. Our computational results suggest that the KIEs in the C–H bond dissociation of ethane are significantly affected by molecular parts that have no direct relevance to the abstraction reaction; the values calculated from transition state theory fall in a range of 7–14 at 300 K. In contrast, the four-centered abstraction is clearly preferred in energy to the direct abstraction in the gas-phase process ($FeO^+ + CH_4 \rightarrow Fe^+ + CH_3OH$) because the iron atom is coordinatively unsaturated. Our current interest is which mechanism is preferred in methane hydroxylation by intermediate **Q** of sMMO; we think that this question can be reduced to whether its diiron active site is coordinatively saturated or unsaturated to allow the Fe···C interaction.

Acknowledgements

This work was supported by a Grant-in-Aid for Scientific Research on the Priority Area 'Molecular Physical Chemistry' from the Ministry of Education, Science, Sports and Culture of Japan and the Iwatani Naoji Foundation's Research Grant. Computations were in part carried out at the Computer Center of the Institute for Molecular Science.

References

[1] P.R. Orates de Montellano (Ed.), Cytochrome P450: Structure, Mechanism, and Biochemistry, 2nd ed., Plenum, New York, 1995.
[2] M. Sono, M.P. Roach, E.D. Coulter, J.H. Dawson, Chem. Rev. 96 (1996) 2841.
[3] A.L. Feig, S.J. Lippard, Chem. Rev. 94 (1994) 759.
[4] B.J. Wallar, J.D. Lipscomb, Chem. Rev. 96 (1996) 2625.

[5] L.M. Hjelmeland, L. Aronow, J.R. Trudell, Biochem. Biophys. Res. Commun. 76 (1977) 541.
[6] J.T. Groves, G.A. McClusky, R.E. White, M.J. Coon, Biochem. Biophys. Res. Commun. 81 (1978) 154.
[7] W.D. Woggon, H. Fretz, J.M. Coxon (Eds.), Advances in Detailed Reaction Mechanism, vol. 2, JAI Press, Greenwich CT, 1992, p. 111.
[8] J.T. Groves, J. Chem. Educ. 62 (1985) 928.
[9] S.-K. Lee, B.G. Fox, W.A. Froland, J.D. Lipscomb, E. Münck, J. Am. Chem. Soc. 115 (1993) 6450.
[10] K.E. Liu, A.M. Valentine, D. Wang, B.H. Huynh, D.E. Edmondson, A. Salifoglou, S.J. Lippard, J. Am. Chem. Soc. 117 (1995) 10174.
[11] L. Shu, J.C. Nesheim, K. Kauffmann, E. Münck, J.D. Lipscomb, L. Que Jr., Science 275 (1997) 515.
[12] H.-H.T. Nguyen, A.K. Shiemke, S.J. Jacobs, B.J. Hales, M.E. Lidstrom, S.I. Chan, J. Biol. Chem. 269 (1994) 14995.
[13] D. Schröder, H. Schwarz, Angew. Chem. Int. Ed. Engl. 29 (1990) 1433.
[14] A. Fiedler, D. Schröder, S. Shaik, H. Schwarz, J. Am. Chem. Soc. 116 (1994) 10734.
[15] D. Schröder, H. Schwarz, Angew. Chem. Int. Ed. Engl. 34 (1995) 1973.
[16] S. Shaik, D. Danovich, A. Fiedler, D. Schröder, H. Schwarz, Helv. Chim. Acta 78 (1995) 1393.
[17] K. Yoshizawa, Y. Shiota, T. Yamabe, Chem. Eur. J. 3 (1997) 1160.
[18] Y. Shiota, K. Yoshizawa, J. Am. Chem. Soc. 122 (2000) 12317 (and references therein).
[19] K. Yoshizawa, T. Ohta, T. Yamabe, Bull. Chem. Soc. Jpn. 71 (1998) 1899.
[20] K. Yoshizawa, A. Suzuki, Y. Shiota, T. Yamabe, Bull. Chem. Soc. Jpn. 73 (2000) 815.
[21] K. Yoshizawa, J. Inorg. Biochem. 78 (2000) 23.
[22] K. Yoshizawa, Y. Shiota, T. Yamabe, J. Am. Chem. Soc. 121 (1999) 147.
[23] K. Yoshizawa, Y. Shiota, T. Yumura, T. Yamabe, J. Phys. Chem. B 104 (2000) 734.
[24] S. Shaik, M. Filatov, D. Schröder, H. Schwarz, Chem. Eur. J. 4 (1998) 193.
[25] F. Ogliaro, N. Harris, S. Cohen, M. Filatov, S.P. de Visser, S. Shaik, J. Am. Chem. Soc. 122 (2000) 8977.
[26] P.E.M. Siegbahn, R.H. Crabtree, J. Am. Chem. Soc. 119 (1997) 3103.
[27] H. Basch, K. Mogi, D.G. Musaev, K. Morokuma, J. Am. Chem. Soc. 121 (1999) 7249.
[28] B.D. Dunietz, M.D. Beachy, Y. Cao, D.A. Whittington, S.J. Lippard, R.A. Friesner, J. Am. Chem. Soc. 122 (2000) 2828.
[29] K. Yoshizawa, Y. Shiota, Y. Kagawa, T. Yamabe, J. Phys. Chem. A 104 (2000) 2552.
[30] K. Yoshizawa, Y. Kagawa, Y. Shiota, J. Phys. Chem. B 104 (2000) 12365.
[31] D.A. McQuarrie, Statistical Thermodynamics, University Science Books, Mill Valley, 1973.
[32] E. Wigner, J. Chem. Phys. 5 (1937) 720.
[33] A.D. Becke, J. Chem. Phys. 98 (1993) 5648.
[34] C. Lee, W. Yang, R.G. Parr, Phys. Rev. B 37 (1988) 785.
[35] J. Daly, Handb. Exp. Pharmacol. 28 (1971) 285.
[36] P.H. Toy, M. Newcomb, P.F. Hollenberg, J. Am. Chem. Soc. 120 (1998) 7719.
[37] K. Yoshizawa, Y. Shiota, T. Yamabe, Organometallics 17 (1998) 2825.
[38] A.A. Shteinman, J. Biol. Inorg. Chem. 3 (1998) 300.
[39] R.J. Deeth, H. Dalton, J. Biol. Inorg. Chem. 3 (1998) 306.
[40] D.A. Whittington, A.M. Valentine, S.J. Lippard, J. Biol. Inorg. Chem. 3 (1998) 307.
[41] P.E.M. Siegbahn, R.H. Crabtree, P. Nordlund, J. Biol. Inorg. Chem. 3 (1998) 314.
[42] K. Yoshizawa, J. Biol. Inorg. Chem. 3 (1998) 318.
[43] A.A. Shteinman, J. Biol. Inorg. Chem. 3 (1998) 325.
[44] J.D. Lipscomb, L. Que Jr., J. Biol. Inorg. Chem. 3 (1998) 331.
[45] M. Merkx, D.A. Kopp, M.H. Sazinsky, J.L. Blazyk, J. Müller, J.J. Lippard, Angew. Chem. Int. Ed. Engl. 40 (2001) 2783.
[46] H. Yuan, M.L.P. Collins, W.E. Antholine, J. Am. Chem. Soc. 119 (1997) 5073.
[47] M. Takeguchi, K. Miyakawa, I. Okura, J. Mol. Catal. A 132 (1998) 145.
[48] B. Wilkinson, M. Zhu, N.D. Priestley, H.-H.T. Nuyen, H. Morimoto, P.G. Williams, S.I. Chan, H.G. Floss, J. Am. Chem. Soc. 118 (1996) 921.
[49] N.D. Priestley, H.G. Floss, W.A. Froland, J.D. Lipscomb, P.G. Williams, H. Morimoto, J. Am. Chem. Soc. 114 (1992) 7561.
[50] J.C. Neshaim, J.D. Lipscomb, Biochemistry 35 (1996) 10240.
[51] A.M. Valentine, S.S. Stahl, S.J. Lippard, J. Am. Chem. Soc. 121 (1999) 3876.
[52] J.I. Manchester, J.P. Dinnocenzo, L.-A. Higgins, J.P. Jones, J. Am. Chem. Soc. 119 (1997) 5069.
[53] K. Yoshizawa, T. Kamachi, Y. Shiota, J. Am. Chem. Soc. 123 (2000) 9806.